REVIEW

doi:10.1038/nature10318

Nuclear export dynamics of RNA–protein complexes

David Grünwald[1], Robert H. Singer[2] & Michael Rout[3]

The central dogma of molecular biology — DNA makes RNA makes proteins — is a flow of information that in eukaryotes encounters a physical barrier: the nuclear envelope, which encapsulates, organizes and protects the genome. Nuclear-pore complexes, embedded in the nuclear envelope, regulate the passage of molecules to and from the nucleus, including the poorly understood process of the export of RNAs from the nucleus. Recent imaging approaches focusing on single molecules have provided unexpected insight into this crucial step in the information flow. This review addresses the latest studies of RNA export and presents some models for how this complex process may work.

Since its first description in electron micrographs[1], our understanding of the nuclear-pore complex (NPC), arguably the largest nanomachine in the cell, has increased steadily. We are now at the point where we have a comprehensive overview of the NPC components and their contribution to its structure, as well as initial insights into the mechanism of NPC assembly and a sound understanding of the principal functions of the NPC[2]. The 100-nm diameter NPC has a core structure consisting of a hollow cylinder embedded in the nuclear envelope, which displays an eight-fold symmetry of about 30 different proteins termed nucleoporins (Nups). The NPC acts as the gateway between the nucleus and the cytoplasm; only those macromolecules carrying specific import and export signals are permitted to pass through the central channel of the NPC, although water and metabolites can pass through freely[3,4]. The NPC consists of several major domains (Fig. 1): the selective central channel, or central transporter region; the core scaffold that supports the central channel; the transmembrane regions; the nuclear basket; and the cytoplasmic filaments[5]. The central channel is filled and surrounded with a distinct class of Nup that has numerous large domains rich in phenylalanine and glycine repeats, termed FG Nups. It is this central channel and the FG Nups that seem sufficient to mediate selective receptor-mediated transport[6,7]. The nuclear basket consists of eight filaments that reach into the nucleoplasm, attached to each other by a ring at the end. Electron microscopy tomographs have shown that filaments extend from this basket into the nucleus[8,9]. The cytoplasmic filaments are less ordered, forming highly mobile molecular rods projecting into the cytoplasm. The reach of NPCs can extend about 100 nm into the nucleus and cytoplasm[10,11].

The transport of molecules through the NPC is restricted by size; below a mass of approximately 60 kDa, macromolecules can passively diffuse across the NPC (albeit slowly, as the molecule approaches the 60 kDa cut-off[12]). The exact cut-off size remains unclear, although several studies have addressed this issue using various sized molecular probes[13–15]. Moreover, even small macromolecules (that is, below this cut-off) also frequently contain a nuclear localization signal that allows usage of the receptor-mediated transport pathways[16]. Hence, to be shipped as cargoes across the NPC, transport signals seem mandatory for almost all macromolecules: nuclear localization sequences (NLSs) for import into the nucleus and nuclear export sequences (NESs) for export. These signals are recognized by transport factors, each with specific signal preferences. Many transport receptors belong to the karyopherin (importin and exportin) families, characterized by a shared α-superhelical structure. Karyopherins can bind to the NLSs or NESs of their cognate cargoes, to the FG Nups and to the GTPase Ran[17]. For NLS-containing proteins, an import cycle starts with the formation of the cargo–karyopherin complex in the cytoplasm, which seems to be the rate-limiting step *in vivo*[18,19], and then proceeds with translocation through the NPC and, finally, disassembly of the complex on the nuclear side by the binding of Ran-GTP to the karyopherin[3,4,17]. This process is driven by a Ran-GTP gradient across the nuclear envelope; Ran cofactors localized to the nucleoplasm and cytoplasm and a Ran-specific nuclear transport factor (NTF2) maintain a high concentration of nuclear Ran-GTP and of cytoplasmic Ran-GDP[3,16]. Protein export has been shown to be governed by very similar principles to the well-studied import machinery. An NES on a cargo is recognized by a cognate karyopherin–Ran-GTP dimer in the nucleus and, after translocation across the NPC, the NES-cargo–karyopherin–Ran-GTP complex is disassembled on the cytoplasmic side, through activation of Ran GTPase activity by cytoplasmic RanGAP, achieving directionality[20,21]. As we discuss below, not all transport factors require Ran, nor belong to the karyopherin family; however, notably, all transport receptors can interact directly with FG Nups[22].

An open question is how transport selectivity is achieved by the available components of the NPC. It is clear that FG Nups are essential *in toto*, not surprisingly given that they are the docking sites of the complex for transport factors. Deletions of individual FG repeat domains in yeast are not overtly harmful; however, various combinations of these deletions are, and there is a critical mass of deletions above which the NPC cannot function[6]. Numerous lines of evidence show that the FG repeat domains are natively unfolded[23,24], and they form a tangle of filaments needed to establish the transport barrier in the central channel of the NPC. Reagents that disrupt this tangle also disrupt transport[25–27].

Models of nucleocytoplasmic transport

Although current models explaining the molecular mechanism of selective nuclear transport differ in their details, they agree that the FG repeat domains in the central channel of the NPC form a dense and dynamic network of filaments that blocks translocation of inert molecules, and that this barrier is overcome with the help of transport receptors[18,25,28–31] (Fig. 2). A common idea in these various models is that the FG repeat domains conspire to produce an unfavourable

[1]Delft University of Technology, Faculty of Applied Sciences, Kavli Institute of NanoScience, Department of Bionanoscience, 2628 CJ Delft, The Netherlands. [2]Department of Anatomy and Structural Biology, Gruss Lipper Biophotonics Center, Albert Einstein College of Medicine, Bronx, New York 10461, USA. [3]The Rockefeller University, 1230 York Avenue, New York, New York 10065, USA.

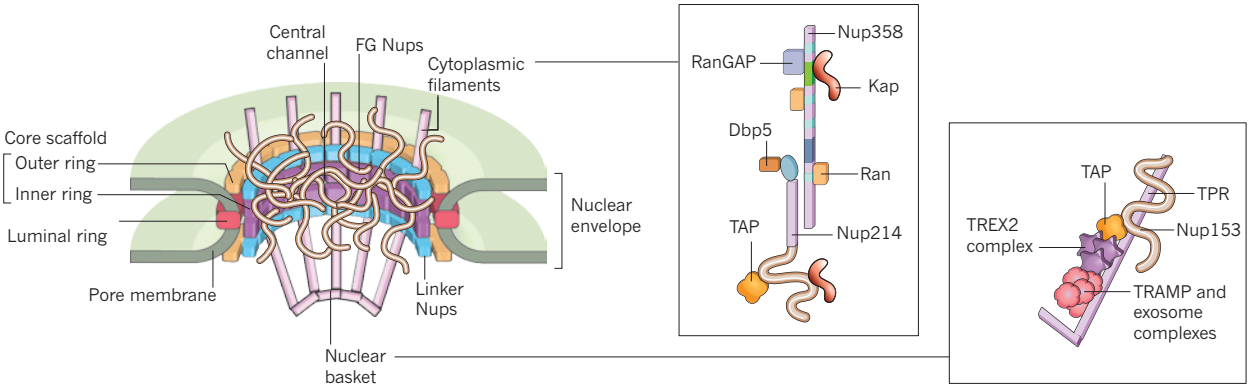

Figure 1 | Nuclear-pore complex basic structure and function. A schematic representation of the NPC. Major structural elements are indicated. The cytoplasmic and nuclear extensions of the vertebrate NPC's periphery are indicated on the cytoplasmic surface as Nup214 and Nup358, which carry factors that aid the egress of cargo such as ribonucleoproteins (RNPs) from the NPC, and on the nuclear surface as TPR (translocated promoter region), the nuclear-basket filament protein that carries factors aiding late RNP processing steps and the first stages of RNP export. See text for more details.

environment for diffusion of inert molecules through the NPC's central channel. This barrier is overcome for cargoes with cognate transport receptors that bind to the FG repeats, thus counteracting the exclusion. In a sense, the NPC can be considered an enzyme for transport, in which only the correct substrates (such as transport factors and their cargoes) can bind to the active site and so pass across the nuclear envelope[28,29]. The directionality of transport is intimately linked to the release of cargo from the transport complex being allowed only on the correct side of the NPC[24–29,31–34].

Transport and single-molecule microscopy

An understanding of the precise steps that are involved in crossing the NPC is still missing. However, emerging single-molecule imaging approaches are showing the real-time dynamics of nuclear transport, and are illuminating its mechanism. Examples of these technologies are 4-Pi microscopy[35,36], single point edge excitation subdiffraction microscopy[37], fluorescence correlation spectroscopy (FCS)[21,38], single-molecule tracking[10,19,39,40] and super-registration microscopy[11] (Box 1). The application of such approaches to determine the distribution of Nups and transport-factor-binding sites supports the notion that the NPC functionally extends far into both compartments (the nucleoplasm and cytoplasm) on either side of itself [8,11,19]. This agrees well with data using colloidal-gold-labelled transport cargoes and electron microscopy, which showed the cargoes docking to filaments extending dozens of nanometres from the NPC[41–43]. Dwell times of transport factors at the NPC have been found to range from 5 to 20 ms (Table 1). Variations in the transport factor, cargo and Ran-GTP concentration have a profound effect on the translocation times of proteins. The dwell time of the karyopherin importin-β1 could be reduced to 1 ms after increased concentrations of unlabelled importin-β1 in the cytoplasmic buffer[44]. In living cells, dwell times were found to be in the range of 5 to 7 ms[19]. Nucleocytoplasmic transport of proteins has been shown by confocal microscopy to be as high as ~1,000 molecules per NPC per second[39,45]. A dwell time of 5 ms translates into 200 parallel transport events per NPC per second, such that as many as 100 copies of importin-β1 occupy each NPC at any one time[46]. Notably, the presence of cargo also has an effect on dwell times by shortening the translocation process[10,44], suggesting that the NPC needs to be viewed as a crowded environment. The central channel of the NPC is presumably filled with disordered FG repeat domains, unloaded and cargo-loaded transport receptors, and non-specific proteins competing to enter the NPC[10,33,34,44] . Molecular crowding can have two effects on NPC function[47,48]: transport times and binding-site availability might change based on the occupation of the central channel with transport factors, cargo and non-specific competitors; and, it might affect the folding or shape of the disordered FG repeat domains[33,34,47,48]. This crowding should lead to competition for space and binding sites; in this way, transport factors with or without their cargoes, binding to the FG repeats, would tend to exclude other proteins that cannot bind in the same way to the NPC. This effect and the constant presence of transport factors in the NPC noted earlier would increase the selectivity of the NPC while maintaining its high flux rate[33,34]. In living cells, this high transport rate is represented by several transport factors carrying many importing and exporting cargoes, including ribonucleoproteins (RNPs). Thus, it seems that it is not the rate of passage across the NPC that limits the speed at which a cell can deliver its cargo from one side of the nuclear envelope to the other; instead, it has been shown that the formation of cargo–receptor complexes is limiting for import[10,18,19,39]. This point will be particularly important for considering how RNPs are delivered across the nuclear envelope.

Notably, the ability to observe single-molecule translocations at the NPC allows the direct measurement of transport efficiencies. As would be expected for a diffusion-based process, only half of the attempts made by NLS cargo to pass from the cytoplasm all the way to the nucleus are successful[39]. Modifications of the importin-β1 concentration, the Ran-GTP gradient and the cargo size have been shown to shift this balance[44,49]. Using fluorescence resonance energy transfer between import receptors and cargo, the directionality and the release of the complex have also been visualized[50]. Transport complexes move by diffusion inside the NPC and thus change their direction stochastically. Hence, cargo release is necessary to impose directionality. Recent FCS data indicated that, unless the cargo is removed from the soluble pool by interaction with immobile structures, the NPC is a bidirectional exchange catalyst, which, according to Le Chatelier's principle, will ultimately establish a steady-state balance of cargo enriched on one side of the nuclear envelope over the other[19,38,50]. This is in agreement with the observation that transport directionality can be inverted based on the direction of the Ran-GTP gradient[11,20,21,49]. The spatial location of cargo–receptor dissociation remains unclear[50]. The distribution of Ran and an importin-β1 truncation with reduced binding affinity for Ran did not indicate a clear location for the release of the receptor–cargo complex[19,36]. For import factors and cargoes, most data indicate that the binding-site distribution along the nuclear–cytoplasmic axis of the central channel is symmetrical, with peaks only a few nanometres off centre compared with the POM121 marker signal (Table 1), although an exception is found for the export of messenger RNA[11] (see below). Tracing single molecules in three dimensions also showed a non-uniform spatial distribution of importin-β1 across the orthogonal axis of the NPC, with higher probability densities found towards the walls of the central channel[37,51]. These and other data suggest that different transport pathways may follow different routes across the NPC[31,52,53].

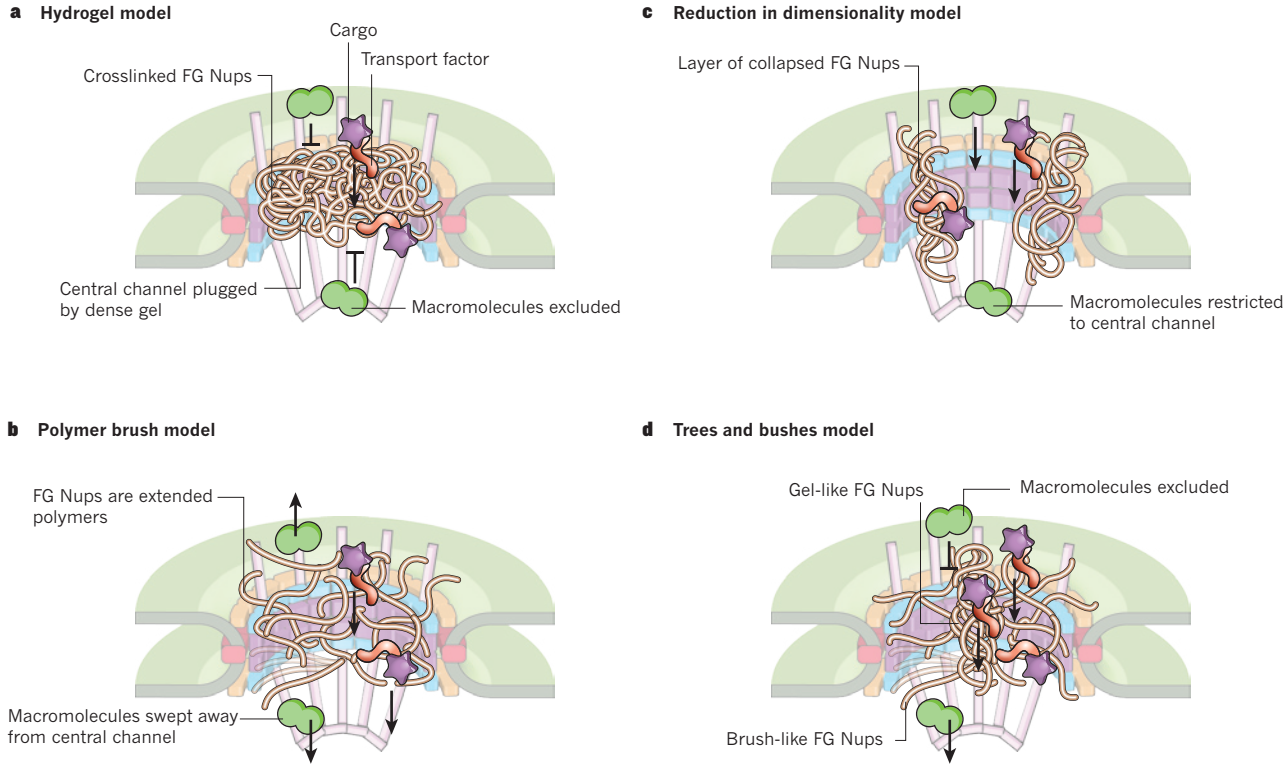

Figure 2 | Modes of transport. Various models for how the FG Nups mediate the selective barrier function of the NPC are shown. The detailed distribution of FG repeat domains is not illustrated here. **a**, FG Nups polymerize into a gel through which transport receptors pass by binding to the FG Nups and dissolving the crosslinks[25]. **b**, The FG repeat filaments diffuse around their tether, and other molecules are excluded from this region. Transport factors pass through by binding to the FG Nups[28,29]. The FG Nups might also act as a molecular brush that collapses once transport receptors have bound other molecules[24]. **c**, FG Nups collapse after binding by transport factors to form a layer along the walls of the channel. This layer is impenetrable to inert molecules but permeable to transport factors[52]. Inert macromolecules are able to pass through the central channel only. **d**, FG Nups form two categories of disordered filaments: collapsed coils, which are gel-like; and extended coils, which are brush-like[31]. Transport factors can pass through both configurations, but macromolecules are excluded. An argument can also be made (not shown) that the central channel *in vivo* will always be permeated with transport receptors, loaded or unloaded with cargo, resulting in a highly crowded environment. This could have a profound influence on the physical state of the FG Nups[33,34].

Principles and players of messenger RNP export

Our picture of nuclear transport is still mainly based on import studies, owing to the difficulty of introducing labelled export substrates into the nucleus. Import cargoes are mostly proteins that have been synthesized in the cytoplasm and are needed in the nucleus. There are also proteins that, once they reach the nucleoplasm, are exported out again by karyopherins such as XPO1 (also known as CRM1). Arguably, however, most export cargoes are RNAs, usually as complexes made of RNA and proteins. The ribosomal subunits and messenger RNPs (mRNPs) are the most abundant of these export cargoes. At around 60 kDa, the average size of protein cargoes is much smaller than mRNP cargoes, which can be as large as 100 MDa[54]. Such extremely large cargoes present a set of unique problems for the nuclear transport machinery (Fig. 3). First, the diameter of these cargoes can considerably exceed the diameter of the NPC central channel. Thus, to pass across the NPC, the quaternary structure of very large RNPs must be remodelled. Second, these cargoes consist of heterogeneous mixes of up to hundreds of molecules of proteins, representing dozens of protein species, packaged around an individual RNA molecule, rather than a single cargo macromolecule. The assembly of the exporting mRNP particle is clearly a complex process. Moreover, the transport machinery must distinguish between immature or incorrectly packaged mRNPs and those that are ready for export[55]. This task is further complicated by the fact that different mRNAs must be packaged into particles with different sizes and compositions. Third, as nucleic acids are in essence extremely long threads, they can potentially experience supercoiling problems, known as tangling.

An explanation of how such cargoes are transported may require additions to the current transport models described above. For example, using electron microscopy to visualize cargo, complexes of up to 39 nm have been shown to cross the NPC; this includes large gold particles that cannot be deformed to squeeze through the central channel. If the gold particles cannot be deformed, then the NPC itself must change shape to accommodate transport of the particles[56]. Another intriguing possibility is that certain NPCs are more specialized for handling the requirements of RNP export. Using immunogold labelling, NTF2 and poly(A)$^+$ mRNAs have been shown to use different sets of NPCs in each nucleus of HL-60 cells[57]. This discrimination may be cell-type specific, as NTF2 has been shown to label NPCs uniformly in HeLa cell nuclei[58]. In yeast, NPCs adjacent to the perinuclear nucleolus lack the proteins myosin-like protein 1 (Mlp1) and Mlp2, which are important for mRNP processing, hinting that mRNP export may avoid these NPCs[59].

One model of choice for RNP export has been that of Balbiani ring mRNA, found in the bloodworm larvae of the midge *Chironomus*. This RNA is huge, up to 40 kilobases (kb), and is packaged into an mRNP particle some 50 nm in diameter, far too large to fit through the NPC unaltered[54,60]. However, classic electron microscopy studies showed that the mRNP unravelled at the nucleoplasmic face of the NPC, and then threaded through as a thin strand while crossing the NPC. These studies, plus immuno-electron microscopy data of the proteins present in the Balbiani ring mRNP at each stage of export, have led to a picture of considerable structural and compositional rearrangement of the transcript during export[54,61,62]. Balbiani ring mRNA seems to be exported at the 5′ end first, making it necessary to postulate a step in transport that orients the mRNA correctly, before it is threaded through the NPC. Live cell data on the mobility and inner nuclear pathways of this giant RNA complex exist, but the export dynamics of this complex remain

BOX 1

Microscopy used for nucleocytoplasmic transport

Fluorescence microscopy has been the standard technology in the field to establish bulk kinetic rates of nuclear transport. In the past five or so years, developments in optical technology have provided the means to use fluorescence microscopy to resolve details in the spatial and kinetic functions of the NPC. This box provides a brief overview of these applications.

Single-molecule tracking (SMT)
In this imaging approach, the diffracted signal of a single molecule can be used to determine the position of the molecule with high precision. In combination with ultrasensitive detection and imaging frame rates of a few milliseconds, individual cargoes and receptor molecules can be followed, and their interaction time with the NPC determined[10,11,38]. The limitations of SMT are that only one species of molecule can be resolved in any spectral channel, and mapping between spectrally resolved channels is still diffraction limited.

Super-registration microscopy
Super registration uses a cellular fiduciary marker to allow measurement of molecular interactions at the nanometre length and millisecond timescale[11].

Single point edge excitation subdiffraction (SPEED) microscopy
In the SPEED method, a highly focused confined excitation beam (similar to confocal microscopy) is combined with ultrasensitive wide-field detection[37]. The resultant data have high signal-to-noise ratios and can be interpreted in three dimensions using data modelling. This approach has been used to track single molecules inside the NPC with virtual three-dimensional subdiffraction resolution.

Highly inclined and laminated optical sheet microscopy (HILO)
In this approach, an analogy to total internal reflection fluorescence (TIRF) microscopy is used to tilt the excitation beam relative to the optical axis of the microscope[46]. Although TIRF is restricted to surface-bound signals within a distance of a few hundred nanometres of the cover glass, HILO can achieve adjustable penetration depth of the sample and provide improved signal-to-noise ratios in the images, allowing SMT and super-registration imaging in the nucleus.

Fluorescence correlation spectroscopy (FCS)
The fluctuation of fluorescence in a fixed confocal excitation spot is analysed to measure diffusive dynamics of the observed molecules[21,35,36]. This has the advantage of being able to resolve fast dynamics, and it has been applied to study the equilibrium conditions of NPC transit at the single-molecule level.

4-Pi microscopy
This approach is an extension of confocal microscopy in which two objectives are placed on opposite sides of the sample, doubling the effective numerical aperture of the detection system[35,36]. After deconvolution of the images, this scanning technology provides excellent resolution along the optical axis of the microscope. The method has been extended to FCS and was used to study the interaction of transport receptors with NPCs. The method also yields good registration between several spectrally resolved images.

Super-resolution microscopy
None of the various super-resolution methods — such as structured illumination microscopy, photo-activation localization microscopy, stochastic optical reconstruction microscopy and stimulated emission depletion imaging — has yet been applied to NPC functional imaging. Ultimately, the further development of these technologies, and technical advances in optics, detectors and also in the design of fluorescent reporters, will result in high-resolution kinetic data of NPC function beyond the current state of the art.

unknown[60]. The ability of conventional electron microscopy to capture so many examples of its transport suggests the rate of passage of the Balbiani ring RNP is relatively slow across the NPC[60]. By contrast, average-sized mRNAs of a few kilobases (such as β-actin) are exported so fast that such major quaternary structural unfolding seems unlikely, although some remodelling must occur (see below)[11]. Even larger mRNAs such as the dystrophin transcript (~10 kb) may require unfolding and export on timescales of only a second[40], providing some perspective on the extreme that the Balbiani ring mRNA probably represents.

Protein import into the nucleus has been shown to be GTP dependent, with directionality imposed by the Ran-GTP gradient leading to dissociation of the transport complex in the nucleus[16]. Although Ran is involved in upstream events leading to export (such as the import of mRNA-processing and mRNA-maturation proteins), it does not seem to provide the direct driving gradient for RNA export, which seems to be ATP dependent[63–68]. How export directionality is ensured is also unclear[69]. It is likely that the host of accessory proteins tethered to the nuclear and cytoplasmic filaments of the NPC (Fig. 1) have important roles in exchanging proteins from the mRNPs as they pass through the NPC, particularly stripping away nuclear transport factors as the mRNP exits the cytoplasmic side of the NPC, and so ensuring that transport is unidirectional. RNP export starts at the nuclear basket, where the TREX2 (3′ repair exonuclease 2), TRAMP (Trf4-Air2-Mtr4p polyadenylation) and exosome complexes, involved in proofreading and final assembly of the RNP before its export, are found hovering[70] (Fig. 1). After processing at the basket, the RNP must then enter the realm of the FG Nups. A key player in this stage is TAP (also known as NXF1), which forms a dimer with p15 (also known as NXT1) — these are homologues of the yeast Mex67–Mtr2 heterodimer — although p15 has been shown to be dispensable for export[71]. These proteins form the major transport receptors for mRNPs, as they bind both the mRNP particles and FG repeats[72–74]. After passing through the central channel, the RNP must then encounter the filaments on the cytoplasmic face of the NPC. Here, Nup214, Nup358 and Dbp5, a DEAD-box helicase, have also been shown to be essential for mRNA export[75–77]. Dbp5 functions in an ATP-dependent manner and has been proposed to supply the motor activity that would provide mechanical force to reshape the mRNP, although this motor function has not yet been conclusively shown[78–80]. A ratchet model has also been proposed for RNA export, in which the Dbp5-mediated removal of TAP–p15 leads to transport directionality[69]. Although remodelling events could be used to prevent mRNA from diffusing back through the central channel into the nucleus[69], the exact point of first interaction between Dbp5 and mRNA is also unclear[81–84]. Specific binding sites for Dbp5 have been identified in Nup214. Because this is a cytoplasmic filament Nup, it places Dbp5 in an ideal position to receive mRNPs as they begin to exit the NPC, and the remodelling function of Nup214 would thus prevent the mRNPs from re-entering. This model was recently supported by crystal structures of the yeast Dbp5–Gle1–Nup159 (Nup214 in mammals) complex that support Dbp5 binding to RNA. Separation of the carboxy- and amino-terminal RecA-like domains of Dbp5 is triggered by Gle1 in

Table 1 | The dynamic range of NPC-mediated transport

Substrate	Dwell time (ms)	Peak centre (nm)	Distribution	Condition	Reference
NTF2	5.8 ± 0.2	−30	Symmetrical	Permeabilized cells	10
NTF2–cargo	5.2 ± 0.2	ND	ND	Permeabilized cells	10
Transportin	7.2 ± 0.3	−2	Symmetrical	Permeabilized cells	10
Transportin–cargo	5.6 ± 0.2	ND	ND	Permeabilized cells	10
Importin-α–cargo (depleted of CAS and GTP)	28 ± 1	ND	ND	Permeabilized cells	50
2×GFP–NLS	10 ± 1	ND	ND	Permeabilized cells, glycerol	39
2×GFP–NLS (depleted of Ran and GTP)	45 ± 5	ND	ND	Permeabilized cells, glycerol	39
2×GFP–NLS (15 mM importin-β)	1.0 ± 0.1	ND	ND	Permeabilized cells, glycerol	44
2×GFP–NLS	7.8 ± 0.4	ND	ND	Living cells, microinjection	44
2×GFP–NLS (competition with dextran)	1.8 ± 0.1	ND	ND	Living cells, microinjection	44
Importin-α–cargo	7.6 ± 0.5	ND	ND	Permeabilized cells	50
Importin-α–cargo (depleted of Ran-GTP)	31 ± 6	ND	ND	Permeabilized cells	50
Ran	10.5 ± 0.8 to 24.8 ± 1.6	−9 ± 82 to −37 ± 82	Symmetrical	Permeabilized cells	36
eGFP	0.4 ± 0.1 to 0.9 ± 0.2	ND	ND	Permeabilized cells	36
BSA	6.2 ± 0.3	−13 ± 1	Symmetrical	Living cells, microinjection	19
Importin-α	7.5 ± 0.8	−6 ± 2	Symmetrical	Living cells, microinjection	19
Importin-β	6.6 ± 0.2*	−10 ± 2	Symmetrical	Living cells, microinjection	19
Importin-β (ΔN44)	11.8 ± 0.6*	−8 ± 1	Symmetrical	Living cells, microinjection	19
Transportin	4.6 ± 0.1*	5 ± 2	Symmetrical	Living cells, microinjection	19
Importin-β	5 ± 2.2	ND	ND	Living cells, microinjection	37
Quantum dots	2 s to 15 min, median 34 s	−5†	Symmetrical	Permeabilized cells	49
Dys mRNA	500	ND	ND	Living cells, MS2 system	40
β-Actin mRNA	180 ± 10	−97 ± 17 to 71 ± 22	Bimodal	Living cells, MS2 system	11

The dwell times for different factors used to probe NPC transport are given. Errors are indicated as published. Where available, the centre of the binding-site distribution along the transport axis is reported, and the shape of that distribution indicated. The peak centre was measured relative to a POM121–fluorescent-marker fusion protein (either POM121–GFP or POM–tandemTomato). Symmetrical refers to shapes that have one peak and roughly similar decays on both sides. Bimodal refers to β-actin mRNA, for which several binding sites have been found. Condition refers to the preparation of cells and buffer conditions, as discussed in the text. BSA, bovine serum albumin; CAS, recycling cofactor for importin-α; *Dys*, dystrophin; eGFP, enhanced green fluorescent protein; GFP, green fluorescent protein; ND, not determined; 2×GFP–NLS is an artificial transport cargo molecule, made from a fusion of two GFP molecules that have an NLS. The MS2 system is a method of visualizing mRNA using a cassette of stem–loops that binds tightly to the MS2 coat protein fused to GFP[11].
*A second component of ~5 to 15% with a significantly longer dwell time was found.
†No POM121 used; peak positions found ~20 nm into the central channel.

an ATP-dependent manner. After RNA release, Dbp5 is bound by Nup159, resulting in a further separation of the RecA-like domains[64]. Inositol hexakisphosphate binding to Gle1 has been shown to be specific and essential for this process, and a single Dbp5 seems to be able to allow multiple cycles of mRNP remodelling[85,86]. DEAD-box helicases are involved in several nuclear processes that lead to the formation of export-competent mRNPs[68,75,87,88]. Taken together, it seems likely that a certain size limit exists above which rearranging of the mRNP before or during export is mandatory. It also seems safe to speculate that, based on the extensive heterogeneity of mRNAs, this size limit is not sharply defined.

The complete protein content of mRNPs is unknown, so the range of composition differences between different mRNPs is still uncharacterized. Which proteins of the mRNP are involved in mediating transport across the NPC and how many of them are exchanged at the NPC remain central questions in the field. Another key issue is whether a common export mechanism exists for all mRNPs or whether there are transcript-specific differences. In addition, mRNA complexes also have pivotal roles in the life cycle of the cell and are therefore controlled by many processing and checkpoint steps, which are now suspected of being NPC coupled[70]. Molecular crowding[47,89], discussed before in the context of the molecular environment within the central channel of the NPC (Fig. 2), also has a profound effect on nuclear structure and so could influence the passage of nascent mRNPs to the NPC[48]. For example, it remains unclear whether access to NPCs is sometimes hindered by chromatin, although current super-resolution microscopy data do not suggest this[11,40,90].

The dynamics of mRNP export

An insight into the effects that large cargoes may have on transport dynamics is based on imaging quantum dots as they are imported through the NPC from the cytoplasm to the nucleoplasm of living cells[49]. Not surprisingly, transport times were found to be long compared with single protein import measurements. Translocation times of 2 s to several minutes, with a median at 34 s, were measured, which are far longer than those found for the export of similarly sized β-actin mRNPs[11,49] (see also below). This can be explained in part by the fact that quantum dots are rigid substrates and, compared with mRNA complexes, lack the ability to reconfigure during transport. It may also point to the idea that the specific machineries recruited to the mRNP are crucial for ensuring its speedy, as well as specific, transit across the NPC.

Recently, a rather more detailed picture comprising docking, translocation and release for mRNA export across the NPC has been presented[11]. Pivotal for the measurement of nanometre-scale distances between mRNA and NPC was super-registration of the two spectrally resolved signals (Fig. 4). By using the NPCs themselves to generate the registration signal, it was possible to super-register the co-localization of single-molecule signals with ~10 nm precision along the nuclear envelope in the living cell[11]. This detailed picture of mRNA export complements that described previously[40], in which a model RNA was transiently expressed and its movement traced in the nucleoplasm and during translocation using single-molecule tracking. The translocation time was estimated to be 1 s, based on the data acquisition rate of 1-s time intervals. On the basis of statistical

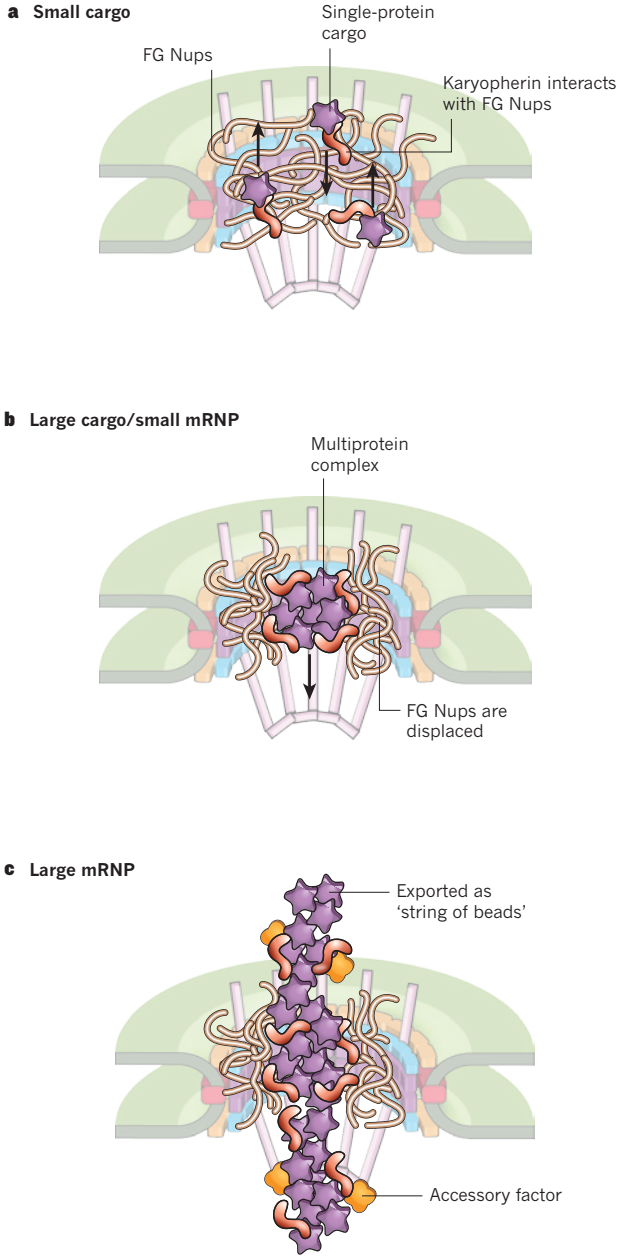

Figure 3 | Transport of cargoes. The challenges faced by the NPC in transporting cargoes of different sizes are shown. Small cargoes are easily accounted for by all existing models (see Fig. 2), but large cargoes raise issues for the functionality of the NPC. **a**, Small cargoes are usually single proteins. They attach to karyopherins, which carry the cargo through the NPC by interacting with the FG Nups. No large-scale displacement of the FG Nups is necessary, and the cargo–karyopherin complexes can be transported bidirectionally. **b**, Large cargoes and RNPs are usually multiprotein complexes that contain several transport factors. Large cargoes displace the FG Nups and sterically hinder other transport. **c**, An mRNP is exported as a 'string of beads', in which each 'bead' behaves as a large cargo. Multiple accessory factors aid in the processing of the mRNP at both the nuclear basket and the cytoplasmic filaments.

analysis of single-molecule tracking data, a diffusion coefficient of ~0.2–0.6 $\mu m^2 s^{-1}$ was calculated, and the translocation velocity given as 0.65 $\mu m s^{-1}$. Complex kinetics were inaccessible owing to limitations in the image-acquisition rate, and details of the export step were not observed with this time resolution, but rather acquired through model-based data analysis. Importantly, despite the different sizes of the mRNAs and the very different data-acquisition timescales (3.3-kb β-actin mRNA imaged with 50 Hz, and 4.8-kb mRNA imaged with 2 Hz), both studies support the rapid transport of mRNAs.

Perhaps the most surprising result to emerge[11] was that a medium-sized endogenous mRNP of about 3 MDa spends most of its transport time of ~200 ms equally between docking and release at the nuclear basket and cytoplasmic filaments, whereas translocation through the central channel itself occurs in a remarkably rapid manner within a time interval of less than 20 ms (Fig. 4). This would correspond to a diffusion coefficient along the central channel of roughly 0.06 $\mu m^2 s^{-1}$ (free diffusion over a 50-nm distance within 10 ms), or a velocity of 5 $\mu m s^{-1}$ (linear movement across the central channel). This compares favourably with transport times for protein cargoes that have been found to range from 1 to 15 ms (corresponding to a diffusion coefficient in the channel of 0.13 $\mu m^2 s^{-1}$, assuming a 5-ms dwell time that is attributed only to the central channel), and with the free diffusion rate of such a 3 MDa cargo[10,11,39,44,60]. Thus, it seems that the export of RNAs is not limited by getting through the central channel of the NPC, but rather by the time taken in preparation for this transport, and conversely its termination from it. This is analogous to protein import, in which the transport step is minor compared with the assembly of the transport-factor–cargo complex[18]. Given the apparent complexity of the assembling, NPC targeting and disassembling of mRNP cargoes (each consisting of up to hundreds of individual molecules), this makes sense. In the quantum dot study[49], these docking and release steps were not observed[49]. This could be explained by a much slower translocation step that 'hid' more complex fast kinetics at the rim of the NPC, but also seems to suggest that transport of mRNPs includes steps to hold the mRNP at the docking and release sites. The rapid transition through the central channel must be taken into account when considering which of the transport models is correct. To achieve these times, a model is needed that allows the barrier forces in the central channel and FG Nup region to be overcome within a very short time. It is also clear from these data that mRNP export was not limited in rate by the translocation step, but rather was dependent on the interaction between the cargo and the peripheral elements (at both the nuclear and the cytoplasmic interfaces). This is an important notion as deletion experiments in yeast have shown that most asymmetrical or peripheral Nups are either redundant or unnecessary to achieve selectivity, although the factors associated with some of these proteins (such as Gle1) are important[6,85]. However, it has been shown in yeast that certain types of FG Nup, and not just those associated with the nuclear basket or cytoplasmic filaments, are crucial for efficient mRNP export[6,91]. This indicates that, as with karyopherin-mediated protein transport, particular kinds of FG Nup cooperate to form specific pathways across the NPC that are favoured by specific types of transport-factor–cargo complex[22].

Export of ribosomes and other RNAs

Our understanding of the mechanisms and dynamics of the export of other RNAs remains sketchy. Other RNAs include those much smaller than typical mRNAs: for example, transfer RNA, microRNA (miRNA) and small nuclear RNA, but also large RNA-containing particles such as viral RNA, ribosomal RNAs and ribosomal subunits[55,92]. Results indicate that the export of small RNAs is similar to the export of proteins and even involves the same or similar karyopherin transport factors[55]. Both tRNAs and miRNAs seem to carry sequences (or structural elements) analogous to NESs that are recognized by their cognate export karyopherins, whereas mature small nuclear RNP complexes have an NES-containing protein recognized by the export karyopherin CRM1 (ref. 55). Ribosomal subunit export is another topic of great interest[92]. Like mRNP export, the export of both the 40S and the 60S ribosomal subunits must be rapid. Although little is known about the export of the 40S subunit, it has been established that the 60S subunit can use many different pathways for export[91]. This has been interpreted as a mechanism to make this a robust process, less sensitive to the cellular stress response or inhibition. However, the overall regulation, transport mechanisms and detailed dynamics of ribosomal export are much less well understood than for mRNP export. One limit here will be devising

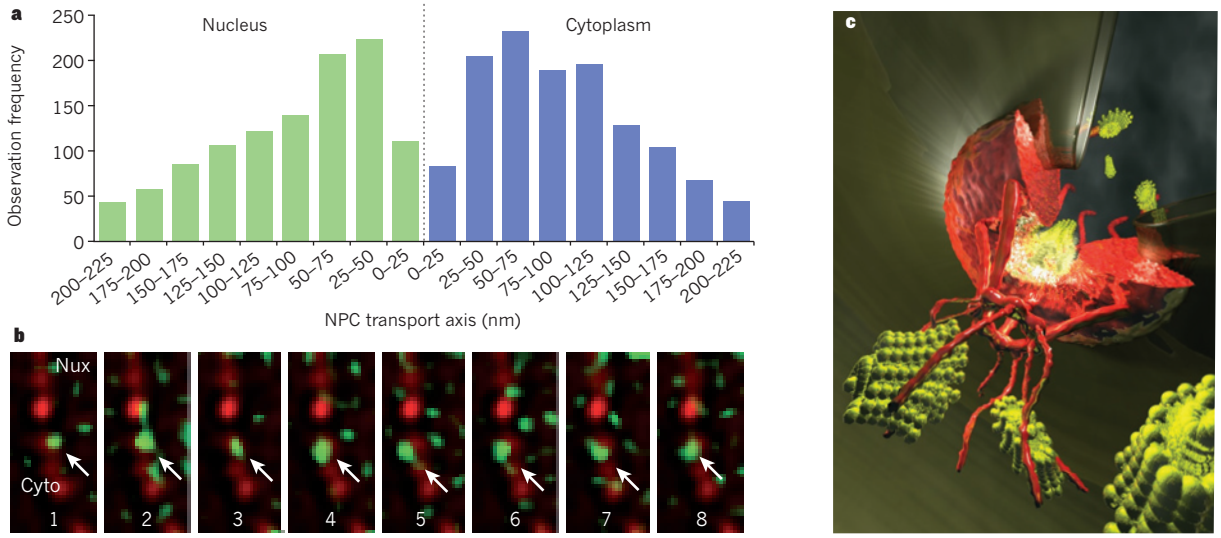

Figure 4 | Imaging of NPC transport events one molecule at a time. **a**, By localizing cargo relative to the NPC, spatially resolved binding sites can be recorded along the transport axis of the NPC. The histogram represents data on β-actin mRNA transport[11]. The zero position (dotted line) is determined by localizing the position that POM121 is fused to a fluorescent marker. The two peaks, one on the nuclear surface and one on the cytoplasmic surface of the NPC, are interpreted as docking and release sites. **b**, An image series from a single mRNP export event showing β-actin mRNA (green) traversing the NPC (red). After docking in the nucleoplasm (Nux) in frame 1, the mRNA (arrows) is repeatedly observed along the NPC until, in frame 8, it reaches the cytoplasm (Cyto). The positions are super-registered to the NPC signal and contribute to the data in **a**. **c**, An artist's impression of a large cargo (green) docking and transiting through the NPC (red). Up to a certain size limit (see text), large cargoes dock to the NPC, transit through the central channel relatively fast, then linger before release. The docking and release steps allow remodelling and/or reorientation of large cargoes. Artwork by Tremani, TU Delft.

a consistent labelling strategy for ribosomal subunits that allows specificity of label targeting to a subclass of 40S or 60S subunits, and stays on the subunits during transport.

Outlook

Recent work provides insight into how cells transport RNPs across the NPC. Although it seems that the constraints of the narrow channel should make export slow, this is not the case. Instead, the cell has specialized structures on the periphery of the NPC that prepare RNPs for a rapid step through its central channel, and for the repackaging of the RNPs for release into the cytoplasm. The relevance of this mechanism probably extends beyond RNPs, because large complexes of proteins may also need to be temporarily restructured for rapid passage.

Much work over the past few decades has been directed at the structure and composition of the NPCs, but with new microscopic approaches it is now possible to overlay this with a kinetic picture, one that is essential to understand the mechanisms involved in transport. Ensemble measurements have not yet been able to describe sufficiently the individual steps of molecular mobility and interaction, spatial–temporal resolution, kinetic parameters and geographical mapping. The ability to study the dynamics of transport processes opens up key questions, such as the role of the peripheral structures of the NPC in transport, because selectivity seems to be mainly achieved in the central channel. Regulatory functions[93], links to diseases[94,95] and the ageing of NPCs[96] have been established for the NPC under *in vivo* conditions and are mediated by either specific Nups or transport receptors. However, the spatial overlay of these processes within the NPC remains unclear. A picture of distinct transport pathways for specific cargo along the central channel of the NPC is emerging[37,51], ultimately leading to the question of whether all NPCs are equal. In single-molecule transport studies only small subsets of NPCs in each experiment show activity[11,19]. β-Actin mRNA was also shown to frequently scan NPCs without engaging in transport. This raises questions addressing NPC activity, such as whether the scanning could be due to certain NPCs (or a specific subpopulation) being inaccessible for mRNA transport, or β-actin mRNA transport specifically. This could result from NPCs being too busy to transport alternative RNA cargoes, or these NPCs could be resting stages, rendering NPCs temporarily inactive. Alternatively, NPCs might be specialized for particular kinds of transport (see above). Another intriguing possibility is that NPCs could reject the passage of mRNPs during a quality-control surveillance step. In yeast, Nup60 has been implicated in a quality-control step for specific mRNAs localized to the bud tip[97]. It has been suggested that the quality control of complex cargoes — for example, nonsense-mediated decay of premature-termination-codon-containing mRNAs — could occur at the NPC[98], although it is unclear whether the process is completed at the NPC or whether the NPC simply initiates it.

Study of the NPC has implications for infectious diseases, as it may be possible to inhibit viruses such as HIV by tampering with cellular transport pathways[99]. Moreover, although it is by far the most extensively used, the NPC may not be the only method of crossing the nuclear envelope: some viruses, for example, seem to bypass the NPC entirely and bud directly from the nucleoplasm to the cytoplasm[100].

A key question in the field is how selectivity in the central channel works and copes with a large variety of cargo sizes, including huge mRNP complexes. The surrounding cellular milieu, and the simultaneous docking to the NPC of multiple transport factors and their large and small cargoes, means that the NPC and its vicinity are very crowded places. Because of this, competition between transport factors, cargoes and non-specific vicinal proteins for space and binding sites must strongly modulate the behaviour of the NPC and RNP export. It will be difficult to completely reproduce all these effects *in vitro*, so the new imaging techniques that have literally shed light on mRNP export will be necessary to understand ultimately how it works. ■

1. Franke, W. W. & Scheer, U. The ultrastructure of the nuclear envelope of amphibian oocytes: a reinvestigation *J. Ultrastruct. Res.* **30,** 288–316 (1970).
2. Walde, S. & Kehlenbach, R. H. The Part and the Whole: functions of nucleoporins in nucleocytoplasmic transport. *Trends Cell Biol.* **20,** 461–469 (2010).
3. Mattaj, I. W. & Englmeier, L. Nucleocytoplasmic transport: the soluble phase. *Annu. Rev. Biochem.* **67,** 265–306 (1998).
4. Pemberton, L. F. & Paschal, B. M. Mechanisms of receptor-mediated nuclear import and nuclear export. *Traffic* **6,** 187–198 (2005).
5. Alber, F. *et al.* The molecular architecture of the nuclear pore complex. *Nature* **450,** 695–701 (2007).

This study describes an approach to combine different experimental data into a common framework with a defined error, underlining the essential features of NPC architecture.
6. Strawn, L. A., Shen, T. X., Shulga, N., Goldfarb, D. S. & Wente, S. R. Minimal nuclear pore complexes define FG repeat domains essential for transport. *Nature Cell Biol.* **6,** 197–206 (2004).
7. Jovanovic-Talisman, T. *et al.* Artificial nanopores that mimic the transport selectivity of the nuclear pore complex. *Nature* **457,** 1023–1027 (2009).
8. Ris, H. & Malecki, M. High-resolution field emission scanning electron microscope imaging of internal cell structures after Epon extraction from sections: a new approach to correlative ultrastructural and immunocytochemical studies. *J. Struct. Biol.* **111,** 148–157 (1993).
9. Kiseleva, E. *et al.* Yeast nuclear pore complexes have a cytoplasmic ring and internal filaments. *J. Struct. Biol.* **145,** 272–288 (2004).
10. Kubitscheck, U. *et al.* Nuclear transport of single molecules: dwell times at the nuclear pore complex. *J. Cell Biol.* **168,** 233–243 (2005).
11. Grünwald, D. & Singer, R. *In vivo* imaging of labelled endogenous β-actin mRNA during nucleocytoplasmic transport. *Nature* **467,** 604–607 (2010).
This is the first study to follow a single mRNA in detail through the NPC, showing that overall transport times are fast, ~hundreds of milliseconds, and that docking and release are visible kinetic steps.
12. Gorlich, D. & Kutay, U. Transport between the cell nucleus and the cytoplasm. *Annu. Rev. Cell Dev. Biol.* **15,** 607–660 (1999).
13. Paine, P. L., Moore, L. C. & Horowitz, S. B. Nuclear envelope permeability. *Nature* **254,** 109–114 (1975).
14. Keminer, O. & Peters, R. Permeability of single nuclear pores. *Biophys. J.* **77,** 217–228 (1999).
15. Mohr, D., Frey, S., Fischer, T., Guttler, T. & Gorlich, D. Characterisation of the passive permeability barrier of nuclear pore complexes. *EMBO J.* **28,** 2541–2553 (2009).
16. Macara, I. G. Transport into and out of the nucleus. *Microbiol. Mol. Biol. Rev.* **65,** 570–594 (2001).
17. Wente, S. R. & Rout, M. P. The nuclear pore complex and nuclear transport. *Cold Spring Harb. Perspect. Biol.* **2,** a000562 (2010).
18. Timney, B. L. *et al.* Simple kinetic relationships and nonspecific competition govern nuclear import rates *in vivo*. *J. Cell Biol.* **175,** 579–593 (2006).
19. Dange, T., Grünwald, D., Grünwald, A., Peters, R. & Kubitscheck, U. Autonomy and robustness of translocation through the nuclear pore complex: a single-molecule study. *J. Cell Biol.* **183,** 77–86 (2008).
20. Nachury, M. V. & Weis, K. The direction of transport through the nuclear pore can be inverted. *Proc. Natl Acad. Sci. USA* **96,** 9622–9627 (1999).
21. Kopito, R. B. & Elbaum, M. Reversibility in nucleocytoplasmic transport. *Proc. Natl Acad. Sci. USA* **104,** 12743–12748 (2007).
22. Terry, L. J. & Wente, S. R. Flexible gates: dynamic topologies and functions for FG nucleoporins in nucleocytoplasmic transport. *Eukaryot. Cell* **8,** 1814–1827 (2009).
23. Denning, D. P., Patel, S. S., Uversky, V., Fink, A. L. & Rexach, M. Disorder in the nuclear pore complex: the FG repeat regions of nucleoporins are natively unfolded. *Proc. Natl Acad. Sci. USA* **100,** 2450–2455 (2003).
24. Lim, R. Y. *et al.* Nanomechanical basis of selective gating by the nuclear pore complex. *Science* **318,** 640–643 (2007).
25. Frey, S., Richter, R. P. & Gorlich, D. FG-rich repeats of nuclear pore proteins form a three-dimensional meshwork with hydrogel-like properties. *Science* **314,** 815–817 (2006).
26. Frey, S. & Gorlich, D. A saturated FG-repeat hydrogel can reproduce the permeability properties of nuclear pore complexes. *Cell* **130,** 512–523 (2007).
27. Eisele, N. B., Frey, S., Piehler, J., Gorlich, D. & Richter, R. P. Ultrathin nucleoporin phenylalanine–glycine repeat films and their interaction with nuclear transport receptors. *EMBO Rep.* **11,** 366–372 (2010).
28. Rout, M. P. *et al.* The yeast nuclear pore complex: composition, architecture, and transport mechanism. *J. Cell Biol.* **148,** 635–651 (2000).
29. Rout, M. P., Aitchison, J. D., Magnasco, M. O. & Chait, B. T. Virtual gating and nuclear transport: the hole picture. *Trends Cell Biol.* **13,** 622–628 (2003).
30. Peters, R. The nanopore connection to cell membrane unitary permeability. *Traffic* **6,** 199–204 (2005).
31. Yamada, J. *et al.* A bimodal distribution of two distinct categories of intrinsically disordered structures with separate functions in FG nucleoporins. *Mol. Cell. Proteomics* **9,** 2205–2224 (2010).
32. Lim, R. Y. *et al.* Flexible phenylalanine-glycine nucleoporins as entropic barriers to nucleocytoplasmic transport. *Proc. Natl Acad. Sci. USA* **103,** 9512–9517 (2006).
33. Zilman, A., Di Talia, S., Chait, B. T., Rout, M. P. & Magnasco, M. O. Efficiency, selectivity, and robustness of nucleocytoplasmic transport. *PLoS Comput. Biol.* **3,** e125 (2007).
34. Zilman, A. *et al.* Enhancement of transport selectivity through nano-channels by non-specific competition. *PLoS Comput. Biol.* **6,** e1000804 (2010).
35. Huve, J., Wesselmann, R., Kahms, M. & Peters, R. 4Pi microscopy of the nuclear pore complex. *Biophys. J.* **95,** 877–885 (2008).
36. Kahms, M., Lehrich, P., Huve, J., Sanetra, N. & Peters, R. Binding site distribution of nuclear transport receptors and transport complexes in single nuclear pore complexes. *Traffic* **10,** 1228–1242 (2009).
37. Ma, J. & Yang, W. Three-dimensional distribution of transient interactions in the nuclear pore complex obtained from single-molecule snapshots. *Proc. Natl Acad. Sci. USA* **107,** 7305–7310 (2010).
In this study, very high spatial resolution is achieved by a combination of confocal excitation with camera detection and modelling of data, supporting the existence of defined cargo transport routes within the NPC.
38. Kopito, R. B. & Elbaum, M. Nucleocytoplasmic transport: a thermodynamic mechanism. *HFSP J.* **3,** 130–141 (2009).
39. Yang, W., Gelles, J. & Musser, S. M. Imaging of single-molecule translocation through nuclear pore complexes. *Proc. Natl Acad. Sci. USA* **101,** 12887–12892 (2004).
40. Mor, A. *et al.* Dynamics of single mRNP nucleocytoplasmic transport and export through the nuclear pore in living cells. *Nature Cell Biol.* **12,** 543–552 (2010).
In this paper, various large exogenous mRNP cargos are followed *in vivo*, and their progress from the transcription site to the NPC is shown to be slow (minutes), whereas nuclear transport is more rapid (seconds).
41. Feldherr, C. M., Kallenbach, E. & Schultz, N. Movement of a karyophilic protein through the nuclear pores of oocytes. *J. Cell Biol.* **99,** 2216–2222 (1984).
42. Dworetzky, S. I. & Feldherr, C. M. Translocation of RNA-coated gold particles through the nuclear pores of oocytes. *J. Cell Biol.* **106,** 575–584 (1988).
43. Richardson, W. D., Mills, A. D., Dilworth, S. M., Laskey, R. A. & Dingwall, C. Nuclear protein migration involves two steps: rapid binding at the nuclear envelope followed by slower translocation through nuclear pores. *Cell* **52,** 655–664 (1988).
44. Yang, W. & Musser, S. M. Nuclear import time and transport efficiency depend on importin β concentration. *J. Cell. Biol.* **174,** 951–961 (2006).
45. Ribbeck, K. & Gorlich, D. Kinetic analysis of translocation through nuclear pore complexes. *EMBO J.* **20,** 1320–1330 (2001).
46. Tokunaga, M., Imamoto, N. & Sakata-Sogawa, K. Highly inclined thin illumination enables clear single-molecule imaging in cells. *Nature Methods* **5,** 159–161 (2008).
This study introduces a careful calibration of a simple light shield technique for fluorescence imaging, and is the first direct visualization of the high occupancy of NPCs with several individual transport receptors *in vivo*.
47. Ellis, R. J. Protein folding — inside the cage. *Nature* **442,** 360–362 (2006).
48. Marenduzzo, D., Finan, K. & Cook, P. R. The depletion attraction: an underappreciated force driving cellular organization. *J. Cell Biol.* **175,** 681–686 (2006).
49. Lowe, A. R. *et al.* Selectivity mechanism of the nuclear pore complex characterized by single cargo tracking. *Nature* **467,** 600–603 (2010).
This paper presents the constraints on large cargo transport for artificial, not deformable, cargo, showing the lower time limit for NPC translocation and the upper limit for cargo diameter.
50. Sun, C., Yang, W., Tu, L. C. & Musser, S. M. Single-molecule measurements of importin α-cargo complex dissociation at the nuclear pore. *Proc. Natl Acad. Sci. USA* **105,** 8613–8618 (2008).
51. Fiserova, J., Richards, S. A., Wente, S. R. & Goldberg, M. W. Facilitated transport and diffusion take distinct spatial routes through the nuclear pore complex. *J. Cell Sci.* **123,** 2773–2780 (2010).
References 37 and 51 use ultrastructural studies and super-fast freezing of samples to capture cargo within the NPC in intact cells, demonstrating that cargo can travel along specific routes in the NPC.
52. Peters, R. Translocation through the nuclear pore complex: selectivity and speed by reduction-of-dimensionality. *Traffic* **6,** 421–427 (2005).
53. Dimitrov, D. I., Milchev, A. & Binder, K. Polymer brushes in cylindrical pores: simulation versus scaling theory. *J. Chem. Phys.* **125,** 34905 (2006).
54. Mehlin, H., Daneholt, B. & Skoglund, U. Translocation of a specific premessenger ribonucleoprotein particle through the nuclear-pore studied with electron-microscope tomography. *Cell* **69,** 605–613 (1992).
55. Köhler, A. & Hurt, E. C. Exporting RNA from the nucleus to the cytoplasm. *Nature Rev. Mol. Cell Biol.* **8,** 761–773 (2007).
56. Akey, C. W. Visualization of transport-related configurations of the nuclear pore transporter. *Biophys. J.* **58,** 341–355 (1990).
57. Iborra, F. J., Jackson, D. A. & Cook, P. R. The path of RNA through nuclear pores: apparent entry from the sides into specialized pores. *J. Cell Sci.* **113,** 291–302 (2000).
58. Siebrasse, J. P. & Kubitscheck, U. Single molecule tracking for studying nucleocytoplasmic transport and intranuclear dynamics. *Methods Mol. Biol.* **464,** 343–361 (2009).
59. Galy, V. *et al.* Nuclear retention of unspliced mRNAs in yeast is mediated by perinuclear Mlp1. *Cell* **116,** 63–73 (2004).
60. Siebrasse, J. P. *et al.* Discontinuous movement of mRNP particles in nucleoplasmic regions devoid of chromatin. *Proc. Natl Acad. Sci. USA* **105,** 20291–20296 (2008).
This careful analysis of RNP mobility within the nucleus demonstrates that different mobility distributions observed for an RNP are best explained by single molecules alternating between tethering and diffusion.
61. Kiseleva, E., Goldberg, M. W., Allen, T. D. & Akey, C. W. Active nuclear pore complexes in *Chironomus*: visualization of transporter configurations related to mRNP export. *J. Cell Sci.* **111,** 223–236 (1998).
62. Soop, T. *et al.* Nup153 affects entry of messenger and ribosomal ribonucleoproteins into the nuclear basket during export. *Mol. Biol. Cell* **16,** 5610–5620 (2005).
63. Dargemont, C. & Kuhn, L. C. Export of mRNA from microinjected nuclei of *Xenopus laevis* oocytes. *J. Cell Biol.* **118,** 1–9 (1992).
64. Montpetit, B. *et al.* A conserved mechanism of DEAD-box ATPase activation by nucleoporins and $InsP_6$ in mRNA export. *Nature* **472,** 238–242 (2011).
This study presents the atomic structures of protein complexes for mRNA and factors that have been implicated in NPC-related export, and provides a model for how the release step of large cargo from the NPC is achieved.
65. Conti, E. & Izaurralde, E. Nucleocytoplasmic transport enters the atomic age. *Curr. Opin. Cell Biol.* **13,** 310–319 (2001).

66. Reed, R. & Hurt, E. A conserved rnRNA export machinery coupled to pre-mRNA splicing. *Cell* **108,** 523–531 (2002).
67. Kota, K. P., Wagner, S. R., Huerta, E., Underwood, J. M. & Nickerson, J. A. Binding of ATP to UAP56 is necessary for mRNA export. *J. Cell Sci.* **121,** 1526–1537 (2008).
68. Carmody, S. R. & Wente, S. R. mRNA nuclear export at a glance. *J. Cell Sci.* **122,** 1933–1937 (2009).
69. Stewart, M. Ratcheting mRNA out of the nucleus. *Mol. Cell* **25,** 327–330 (2007).
70. Rodriguez-Navarro, S. & Hurt, E. Linking gene regulation to mRNA production and export. *Curr. Opin. Cell Biol.* **23,** 302–309 (2011).
71. Braun, I. C., Herold, A., Rode, M. & Izaurralde, E. Nuclear export of mRNA by TAP/NXF1 requires two nucleoporin-binding sites but not p15. *Mol. Cell. Biol.* **22,** 5405–5418 (2002).
72. Segref, A. *et al.* Mex67p, a novel factor for nuclear mRNA export, binds to both poly(A)$^+$ RNA and nuclear pores. *EMBO J.* **16,** 3256–3271 (1997).
73. Li, Y. *et al.* An intron with a constitutive transport element is retained in a *Tap* messenger RNA. *Nature* **443,** 234–237 (2006).
74. Hutten, S. & Kehlenbach, R. H. CRM1-mediated nuclear export: to the pore and beyond. *Trends Cell Biol.* **17,** 193–201 (2007).
75. Schmitt, C. *et al.* Dbp5, a DEAD-box protein required for mRNA export, is recruited to the cytoplasmic fibrils of nuclear pore complex via a conserved interaction with CAN/Nup159p. *EMBO J.* **18,** 4332–4347 (1999).
76. Forler, D. *et al.* RanBP2/Nup358 provides a major binding site for NXF1-p15 dimers at the nuclear pore complex and functions in nuclear mRNA export. *Mol. Cell. Biol.* **24,** 1155–1167 (2004).
77. Weirich, C. S. *et al.* Activation of the DExD/H-box protein Dbp5 by the nuclear-pore protein Gle1 and its coactivator $InsP_6$ is required for mRNA export. *Nature Cell Biol.* **8,** 668–676 (2006).
78. Hodge, C. A., Colot, H. V., Stafford, P. & Cole, C. N. Rat8p/Dbp5p is a shuttling transport factor that interacts with Rat7p/Nup159p and Gle1p and suppresses the mRNA export defect of xpo1-1 cells. *EMBO J.* **18,** 5778–5788 (1999).
79. Lund, M. K. & Guthrie, C. The DEAD-box protein Dbp5p is required to dissociate Mex67p from exported mRNPs at the nuclear rim. *Mol. Cell* **20,** 645–651 (2005).
80. Linder, P. mRNA export: RNP remodeling by DEAD-box proteins. *Curr. Biol.* **18,** R297–R299 (2008).
81. Zhao, J., Jin, S. B., Bjorkroth, B., Wieslander, L. & Daneholt, B. The mRNA export factor Dbp5 is associated with Balbiani ring mRNP from gene to cytoplasm. *EMBO J.* **21,** 1177–1187 (2002).
82. Cole, C. N. & Scarcelli, J. J. Transport of messenger RNA from the nucleus to the cytoplasm. *Curr. Opin. Cell Biol.* **18,** 299–306 (2006).
83. Bolger, T. A., Folkmann, A. W., Tran, E. J. & Wente, S. R. The mRNA export factor Gle1 and inositol hexakisphosphate regulate distinct stages of translation. *Cell* **134,** 624–633 (2008).
84. von Moeller, H., Basquin, C. & Conti, E. The mRNA export protein DBP5 binds RNA and the cytoplasmic nucleoporin NUP214 in a mutually exclusive manner. *Nature Struct. Mol. Biol.* **16,** 247–254 (2009).
85. Alcazar-Roman, A. R., Bolger, T. A. & Wente, S. R. Control of mRNA export and translation termination by inositol hexakisphosphate requires specific interaction with Gle1. *J. Biol. Chem.* **285,** 16683–16692 (2010).
86. Noble, K. N., Tran, E. J., Alcázar-Román, A. R., Hodge, C. A., Cole, C. N. & Wente, S. R. The Dbp5 cycle at the nuclear pore complex during mRNA export II: nucleotide cycling and mRNP remodeling by Dbp5 are controlled by Nup159 and Gle1. *Genes Dev.* **25,** 1065–1077 (2011).
87. Gatfield, D. *et al.* The DExH/D box protein HEL/UAP56 is essential for mRNA nuclear export in *Drosophila*. *Curr. Biol.* **11,** 1716–1721 (2001).
88. Stutz, F. & Izaurralde, E. The interplay of nuclear mRNP assembly, mRNA surveillance and export. *Trends Cell Biol.* **13,** 319–327 (2003).
89. Ellis, R. J. Macromolecular crowding: an important but neglected aspect of the intracellular environment. *Curr. Opin. Struct. Biol.* **11,** 114–119 (2001).
90. Schermelleh, L. *et al.* Subdiffraction multicolor imaging of the nuclear periphery with 3D structured illumination microscopy. *Science* **320,** 1332–1336 (2008). **Using fixed cells, this work gives a first glance at the possible contributions of super-resolution microscopy, providing high-resolution images of nuclear structure and showing how NPCs may be made accessible for large cargo.**
91. Terry, L. J. & Wente, S. R. Nuclear mRNA export requires specific FG nucleoporins for translocation through the nuclear pore complex. *J. Cell Biol.* **178,** 1121–1132 (2007).
92. Lo, K. Y. & Johnson, A. W. Reengineering ribosome export. *Mol. Biol. Cell* **20,** 1545–1554 (2009).
93. Shitashige, M. *et al.* Regulation of Wnt signaling by the nuclear pore complex. *Gastroenterology* **134,** 1961–1971 (2008).
94. Alvisi, G., Rawlinson, S. M., Ghildyal, R., Ripalti, A. & Jans, D. A. Regulated nucleocytoplasmic trafficking of viral gene products: a therapeutic target? *Biochim. Biophys. Acta* **1784,** 213–227 (2008).
95. Hurt, J. A. & Silver, P. A. mRNA nuclear export and human disease. *Dis. Model Mech.* **1,** 103–108 (2008).
96. D'Angelo, M. A., Raices, M., Panowski, S. H. & Hetzer, M. W. Age-dependent deterioration of nuclear pore complexes causes a loss of nuclear integrity in postmitotic cells. *Cell* **136,** 284–295 (2009).
97. Powrie, E. A., Zenklusen, D. & Singer, R. H. A nucleoporin, Nup60p, affects the nuclear and cytoplasmic localization of *ASH1* mRNA in *S. cerevisiae*. *RNA* **17,** 134–144 (2010).
98. Isken, O. & Maquat, L. E. Quality control of eukaryotic mRNA: safeguarding cells from abnormal mRNA function. *Genes Dev.* **21,** 1833–1856 (2007).
99. Satterly, N. *et al.* Influenza virus targets the mRNA export machinery and the nuclear pore complex. *Proc. Natl Acad. Sci. USA* **104,** 1853–1858 (2007).
100. Lee, C. P. & Chen, M. R. Escape of herpesviruses from the nucleus. *Rev. Med. Virol.* **20,** 214–230 (2010).

Acknowledgements We apologize to those colleagues whose work, through space considerations, could not be discussed or cited in this review. This work has been supported by funds from the Kavli Foundation to D.G., National Institutes of Health grants GM86217 and GM84364 to R.H.S., and GM062427, RR022220 and GM071329 to M.R. We thank A. Joseph for critically reading the manuscript.

Author Information Reprints and permissions information is available at www.nature.com/reprints. The authors declare no competing financial interests. Readers are welcome to comment on the online version of this article at www.nature.com/nature. Correspondence should be addressed to R.H.S. (robert.singer@einstein.yu.edu).